Nonlinear Estimation of Transient Flow Field Low Dimensional States Using Artificial Neural Nets

Article *in* Expert Systems with Applications · January 2012

DOI: 10.1016/j.eswa.2011.07.135

CITATIONS
6

READS
52

5 authors, including:

Kelly Cohen
University of Cincinnati
214 PUBLICATIONS **1,035** CITATIONS
SEE PROFILE

Stefan Siegel
Atargis Energy Corporation
108 PUBLICATIONS **869** CITATIONS
SEE PROFILE

Jurgen Seidel
United States Air Force Academy
69 PUBLICATIONS **167** CITATIONS
SEE PROFILE

Expert Systems with Applications 39 (2012) 1264–1272

Contents lists available at SciVerse ScienceDirect

Expert Systems with Applications

journal homepage: www.elsevier.com/locate/eswa

Nonlinear estimation of transient flow field low dimensional states using artificial neural nets

Kelly Cohen [a], Stefan Siegel [b], Jürgen Seidel [b], Selin Aradag [c,*], Thomas McLaughlin [b]

[a] Department of Aerospace Engineering, University of Cincinnati, Cincinnati, OH, USA
[b] Department of Aeronautics, United States Air Force Academy, CO 80840, USA
[c] Department of Mechanical Engineering, TOBB University of Economics and Technology, Ankara 06560, Turkey

ARTICLE INFO

Keywords:
Turbulent cylinder wake
ANNE
Low dimensional modeling
DPOD
Flow control

ABSTRACT

Feedback flow control of the wake of a circular cylinder at a Reynolds number of 100 is an interesting and challenging benchmark for controlling absolute instabilities associated with bluff body wakes. A two dimensional computational fluid dynamics simulation is used to develop low-dimensional models for estimator design. Actuation is implemented as displacement of the cylinder normal to the flow. The estimation approach uses a low dimensional model based on a truncated 6 mode Double Proper Orthogonal Decomposition (DPOD) applied to the streamwise velocity component of the flow field. Sensor placement is based on the intensity of the resulting spatial modes. A non-linear Artificial Neural Network Estimator (ANNE) was employed to map the velocity data to the mode amplitudes of the DPOD model. For a given four sensor configuration, developed using a previously validated strategy, ANNE performed better than two state-of-the-art approaches, namely, a Quadratic Stochastic Estimator (QSE) and a Linear Stochastic Estimator with time delays (DSE).

1. Introduction

One of the main purposes of flow control is the improvement of aerodynamic characteristics of air vehicles and munitions enabling augmented mission performance. An important area of flow control research involves the phenomenon of vortex shedding in the wake behind bluff bodies where the flow separates from the surface of the bluff body. Shedding of counter-rotating vortices is observed in the wake of a two-dimensional cylinder above a critical Reynolds number of $Re_c \sim 47$, non-dimensionalized with respect to freestream velocity and cylinder diameter. This phenomenon is often referred to as the von Kármán vortex street, shown schematically in Fig. 1. The vortex shedding leads to a sharp rise in drag, noise and fluid-induced vibration (Gillies, 1998; Koopmann, 1967). The ability to control the wake of a bluff body could be used to reduce drag, increase mixing and heat transfer, and enhance combustion (Park, Ladd, & Hendricks, 1993; Roussopoulos, 1993).

The Reynolds number regime studied in this effort, $Re \sim 100$, corresponds to a range in which the wake is laminar and two-dimensional (Williamson, 1996). When active open-loop forcing of the wake is employed, the vortices in the wake can be "locked" to the forcing signal. This also strengthens the vortices and consequently increases the drag. As opposed to the open-loop approach, in this effort, the unsteady wake is controlled using a feedback controller. The feedback control law is designed using a reduced order model of the unsteady flow. A common method used to substantially reduce the order of the model is Proper Orthogonal Decomposition (POD). This method, as detailed in Holmes, Lumley, and Berkooz (1996), is an optimal approach in that it will capture the largest amount of the flow energy in the fewest modes of any decomposition of the flow. The two dimensional POD method was used to identify the characteristic features, or modes, of a cylinder wake as demonstrated by Noack, Tadmor, and and Morzynski (2004). A common approach referred to as "the method of snapshots" introduced by Sirovich (1987) is employed to generate the basis functions of the POD modes from flow-field information obtained using either experiments or numerical simulations. Cohen, Siegel, and Mclaughlin (2004) Siegel, Cohen, and Mclaughlin (2006) have shown that a low dimensional model of the cylinder wake flow, developed by Gillies[1], can be successfully controlled using a relatively simple linear control approach based on the most dominant mode only. Recently, Siegel, Cohen, Seidel, and Mclaughlin (2006b) developed an extension to the POD approach, referred to as 'Double Proper Orthogonal Decomposition' (DPOD), in which shift modes have been added to account for the changes in the flow due to transient forcing.

For low-dimensional control schemes to be implemented, a real-time estimation of the modes present in the wake is necessary, since it is not possible to measure them directly, especially

* Corresponding author.
E-mail address: selinaradag@gmail.com (S. Aradag).

0957-4174/$ - see front matter © 2011 Elsevier Ltd. All rights reserved.
doi:10.1016/j.eswa.2011.07.135

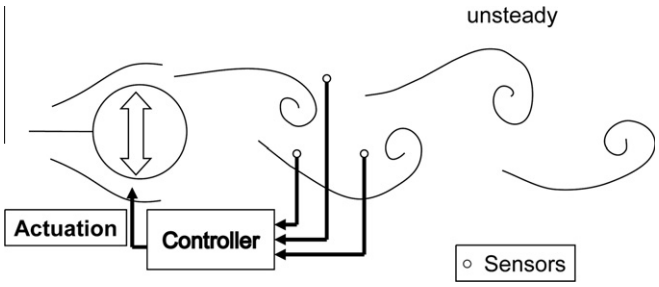

Fig. 1. Schematic of feedback control system setup.

in real-time. The requirement for the estimation scheme then is to behave as a modal filter that combs out the higher modes. The main aim of this approach is thereby to circumvent the destabilizing effects of observation spillover. Spillover has been the cause for instability in the control of spatio-temporal systems and modal filtering was found to be an effective remedy as discussed in detail by Cohen et al. (2004). The intention of the proposed strategy is that the signals, provided by a certain configuration of sensors placed in the wake, are processed by the estimator to provide the estimates of the required mode amplitudes. Pioneering work for providing estimation schemes based on the linear stochastic estimation (LSE) procedure was introduced by Adrian (1977). The linear stochastic estimation of POD modes was successfully implemented by Cohen et al. (2004) for estimation of the POD mode amplitudes for an unforced circular cylinder at low Reynolds numbers. A major design challenge lies in finding an appropriate number of sensors and their locations that will best enable the desired modal filtering. For the closed-loop control of a cylinder wake, the measurement equation has been developed using the LSE method for mapping of measured sensor signals onto the POD mode amplitude required for feedback using a linear measurement matrix. Although this approach is simple and easy to implement, it is important to develop mapping strategies that require fewer sensors.

Velocity field data, provided from either simulation or experiment, is fed into the DPOD procedure. The time histories of the mode amplitudes of the DPOD model are determined by mapping the unforced flow onto the spatial modes using a least squares technique. Sensor measurements may take the form of wake velocity measurements, as in this effort, or, for an application, can be based on surface-mounted pressure measurements and/or shear stress sensors. Then, the estimation of the low-dimensional states is provided using a nonlinear system identification approach (Nelles, 2001) using Artificial Neural Networks (ANN) and ARX (Autoregressive, eXternal input) models (Ljung, 1999; Nørgaard, Ravn, Poulsen, & Hansen, 2003). For the application of the multilayer perception to the multi input and multi output system, the integrated ANN/ARX forms the basis for the algorithm used in the Artificial Neural Network Estimator (ANNE). First, based on an adequate training set, the ANN network is designed and then the "frozen" ANN is validated with new data.

The estimation scheme developed in this effort is based on an artificial neural network, ANNE, designed to provide a non-linear dynamic mapping as opposed to the static linear mapping in a LSE scheme. Recently, other non-linear techniques have been introduced such as the quadratic stochastic estimation (QSE) proposed by Murray and Ukeiley (2002) as well as by Ausseur, Pinier, Glauser, Higuchi, and Carlson (2006) as well as introduction of time delays to the LSE, referred to as DSE in this paper, as examined by Debiasi et al. (2006).

The main objective of this research effort is to develop a systematic approach for the above mapping based on ANNE and subsequently demonstrate the effectiveness of the developed methodology for estimating the state of a circular cylinder wake subjected to transient forcing conditions. It is demonstrated that this method provides desired robustness and system performance. Prediction estimates obtained using ANNE are compared to QSE and DSE. Comparisons are not made to the LSE technique since this technique, although examined, did not provide feasible estimates. Studies are then conducted in order to compare the performance of ANNE to other current state-of-the-art techniques for estimation which have recently emerged in feedback flow control related literature. It is to be noted that the scope of this paper does not include control law development and other closed-loop control studies.

The remainder of the paper is structured as follows: Section s2 describes the numerical simulation of the Navier–Stokes equations, using the Cobalt CFD solver (Strang, Tomaro, & Grismer, 1999). This is followed by a short description of the DPOD procedure in Section 3. Section 4 provides a description of the architecture of ANNE. Section 5 demonstrates how the mode amplitudes of the DPOD model can be estimated from sensor readings using ANNE and results are compared to the QSE and DSE estimation techniques. Section 6 provides conclusions of the current research and finally Section 7 provides the outlook for future work.

2. Computational fluid dynamics simulation

Numerical simulations were conducted with Cobalt Solutions' COBALT solver V.2.02 for direct numerical solution of the Navier–Stokes equations with second order accuracy in time and space. An unstructured two-dimensional grid with 63,700 nodes and 31,752 elements was used. The grid extended from –16.9 cylinder diameters to 21.1 cylinder diameters in the x (streamwise) direction, and ±19.4 cylinder diameters in the y (flow normal) direction. Additional simulation parameters are as follows:

Cylinder diameter $D = 1$ m
Mean flow $U = 34$ m/s
Pressure $P = 4.337$ Pascal
Density $\rho = 5.25 \cdot 10^{-5}$ kg/m^3
Reynolds Number Re = 100
Time step, $\Delta t = 0.00147$ s.
Non-dimensional time step $\Delta t^* = \Delta t \cdot U/D = 0.05$
3 Newton sub-iterations
Damping Coefficients: Advection = 0.01, Diffusion = 0.00
Laminar Navier–Stokes equations, ideal gas
Vortex shedding frequency $f = 5.55$ Hz.

For validation of the computations of the unforced cylinder wake at Re = 100, the resulting value of the mean drag coefficient, C_d, was compared to experimental and computational investigations reported in the literature. Experimental data reported by Oertel (1990) and Panton (1996) point to $C_d$values between 1.26 and 1.4. Furthermore, Min and Choi (1999) report on several numerical studies that obtained drag coefficients between 1.34 and 1.35. The current simulations yield $C_d = 1.35$, which compares well with the reported literature. Another important benchmark parameter is the non-dimensional shedding frequency (Strouhal number, $St = f \cdot D/U$) for the unforced cylinder wake. Experimental results presented by Williamson (1996) point to values of 0.167–0.168. The computations used in this effort result in St = 0.163, which also compares well with the reported literature.

The aim of the current study is to develop an effective estimator of the low-dimensional states based upon flow-field velocity readings when subject to various forcing inputs within the lock-in

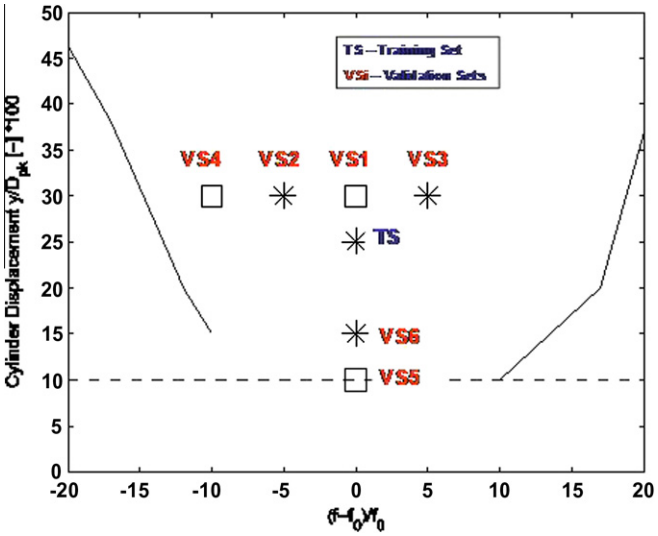

Fig. 2. CFD simulation data sets used for mode set derivation and mode set verification. Note: Solid lines indicate the limits of the Lock-In boundary as identified by Koopmann (1967).

region, where the frequency of the vortex shedding is identical to the forcing frequency. The emphasis is on the robustness of the estimation for off-design cases as depicted in Fig. 2. Seven different data sets, as marked in Fig. 2, for the open loop forced cases were obtained using forcing amplitudes of 10, 15, 25 and 30% cylinder displacement. Some of the cases use a 5–10% lower or higher frequency at 30% displacement, which is still within the lock-in region. The 25% cylinder displacement sinusoidal forcing serves as design point for model development (Design Case "TS"). On the other hand, the off-design cases, VS1-VS5, are utilized for model validation. In Fig. 2, "Koopman" refers to experimental data described in his paper (1967), whereas the CFD data was generated using simulations described earlier in this section.

3. Proper Orthogonal Decomposition (POD) Modeling

POD is an efficient means to reduce spatially highly complex flow fields by representing them by a small number of spatial modes and their mode amplitudes (Noack et al., 2004). Eq. (1) shows this decomposition,

$$u(x,y,t) = \sum_{k=1}^{K} a_k(t)\phi_k(x,y), \tag{1}$$

where a flow quantity u is represented by the spatial modes $\phi_k(x,y)$ and mode amplitudes $a_k(t)$. While this decomposition is well suited to time periodic flow fields, it faces problems for transient flows (Siegel, Cohen, Seidel, & Mclaughlin, 2005). Different additions to the basic POD procedure have been proposed, most notably the addition of a shift mode as introduced independently by Noack, Afanasiev, Morzynski, and Thiele (2003) as well as Siegel et al. (2006b)

This shift mode originally only addressed changes to the mean flow, but the concept has been extended recently by Siegel et al. (2006b) to adjust the fluctuating modes of transient flows as well. This modified POD procedure, referred to as Double POD (DPOD), provides shift modes for all main modes of a transient flow field. A pictorial representation of the DPOD procedure is given in Fig. 3. Starting in the top left corner, the data is split into K bins and each bin is used as an input data set for its individual POD procedure. The resulting SPOD (Short Time POD) modes are then collected across the *bins* and POD is applied again to obtain the shift modes. The procedure is expressed mathematically in Eq. (2), where the index i refers to the main (SPOD) modes of the first POD procedure, while the index j identifies the shift mode order,

$$u(x,y,t) = \sum_{i=1}^{I}\sum_{j=1}^{J} \alpha_{ij}(t)\Phi_{ij}(x,y). \tag{2}$$

The mean flow mode $M_{1,1}$ contains most of the energy, followed by the unsteady von Kármán modes, $M_{2,1}$ and $M_{3,1}$,. This DPOD formulation extends the original concept of the "shift mode": we can now develop a "shift mode", even a series of higher order shift modes, for

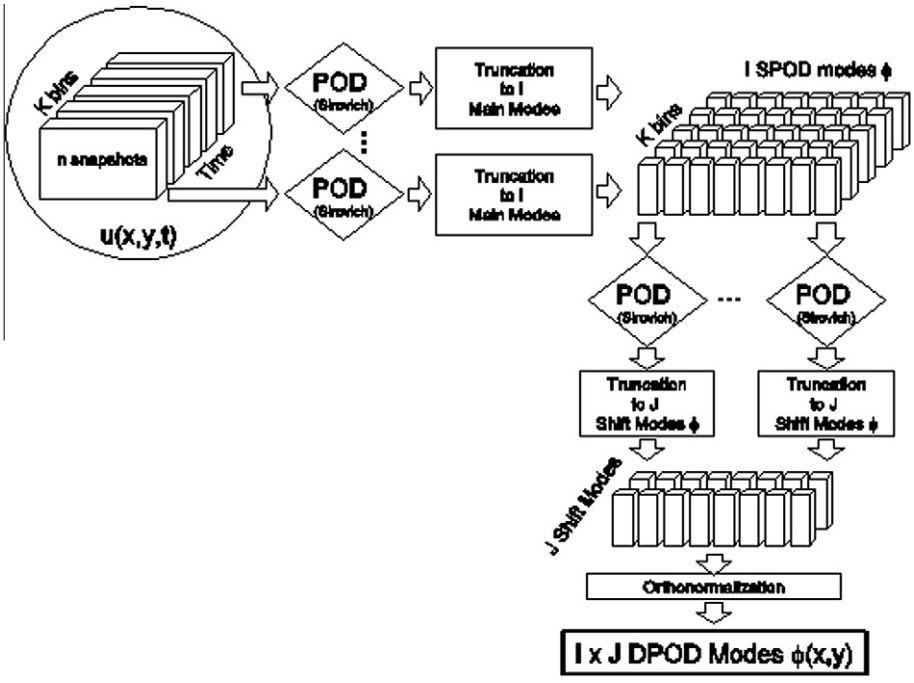

Fig. 3. Flow chart of DPOD decomposition process.

Table 1
Locations of the 4 sensors in the single sensor configurations studied.

Number of sensors in sensor configuration	Non-dimensionalized location of sensor x/D	Non-dimensionalized location of sensor y/D	Targeted mode of each sensor
4	2.0	−0.5	Mode 2,1 & Mode 3,2
4	1.0	−0.5	Mode 3,1 & Mode 2,2
4	1.5	0.0	Mode 1,1 & Mode 1,2
4	3.0	1.5	Mode 3,1 & Mode 2,2

all main modes i. The resulting mode set can be truncated in both i and j, leading to a mode ensemble that is $I_M \times J_M$ in size. After orthonormalization, the decomposition is again optimal in the sense of POD. In the limit of $J = 1$, the original POD decomposition is recovered. While the different modes distinguished by the index i remain the main modes described above, the index j identifies the transient changes of these main modes: For $J > 1$, the energy optimality of the POD decomposition in that direction leads to modes that are the optimum decomposition of a given main mode as it evolves throughout a transient data set. If $J = 2$, then modes $\sigma_{1,1}$ and $\sigma_{1,2}$ are the mean flow and its "shift mode" or "mean flow mode" as described by Noack et al. (2003) and Siegel et al. (2005) , respectively. Thus the modes with indices $j > 1$ can be referred to as first, second and higher order "shift" modes that allow the POD mode ensemble to adjust for changes in the spatial modes. We will refer to all of these additional modes obtained by the DPOD decomposition as shift modes, since they modify a given main mode to match a new flow state due to either a recirculation zone length or formation length change.

These changes may be due to effects of forcing, a different Reynolds number, feedback or open loop control or similar events. Thus, in the truncated DPOD mode ensemble for each main mode, one or more shift modes may be retained based on inspection of energy content or spatial structure of the mode.

The feedback control system developed for the circular cylinder wake problem introduces a control input, y_{cyl}, which moves the cylinder vertically as illustrated in Fig. 1. The flow response is measured using velocity sensors placed in the cylinder wake (Siegel et al., 2006b). This approach is viable for computational studies as well as experimental investigations in a wind or water tunnel. For airborne applications, surface mounted sensors that measure skin-friction[21] or pressure (Cohen, Siegel, Seidel, & Mclaughlin, 2006) have been found to be effective for estimation of the mode amplitudes of the mean flow, $\alpha_{1,1}$, and the fundamental von Kármán POD periodic modes, $\alpha_{2,1}$ and $\alpha_{3,1}$. An estimator is required to accurately map the measured velocities in the wake or surface pressures to estimate DPOD mode amplitudes. Once the truncated state is estimated, a full state controller can then provide an appropriate command for movement of the cylinder. The effectiveness of ANNE compared to other state-of-the-art estimation techniques is detailed in Shin, Cohen, Siegel, Seidel, and Mclaughlin, 2006 for the unforced circular cylinder case at Re = 100 and experimentally validated in Cohen, Siegel, Seidel, and Mclaughlin (2006b) for the sinusoidal forcing of a circular cylinder at Re = 20,000. In this effort, we investigate the ability of the developed estimation schemes to provide estimates for the more complex yet important case when the flow undergoes transient changes to due starting or stopping of sinusoidal forcing.

4. Artificial Neural Network Estimator (ANNE)

The time histories of the mode amplitudes of the DPOD model are determined by mapping the flow field data from a set of sensors onto the spatial modes using one of the estimation techniques described in detail in Cohen, Siegel, Seidel, Aradag, and Mclaughlin (2007). The intent of the proposed strategy is that the velocity measurements provided by the sensors are processed by the estimator to provide the estimates of the six most energetic modes of the DPOD model. The issue of sensor placement and number has been dealt with in detail by Cohen, Siegel, and Mclaughlin (2006c) for the case of a circular cylinder and in this effort a similar strategy for determination of the sensor

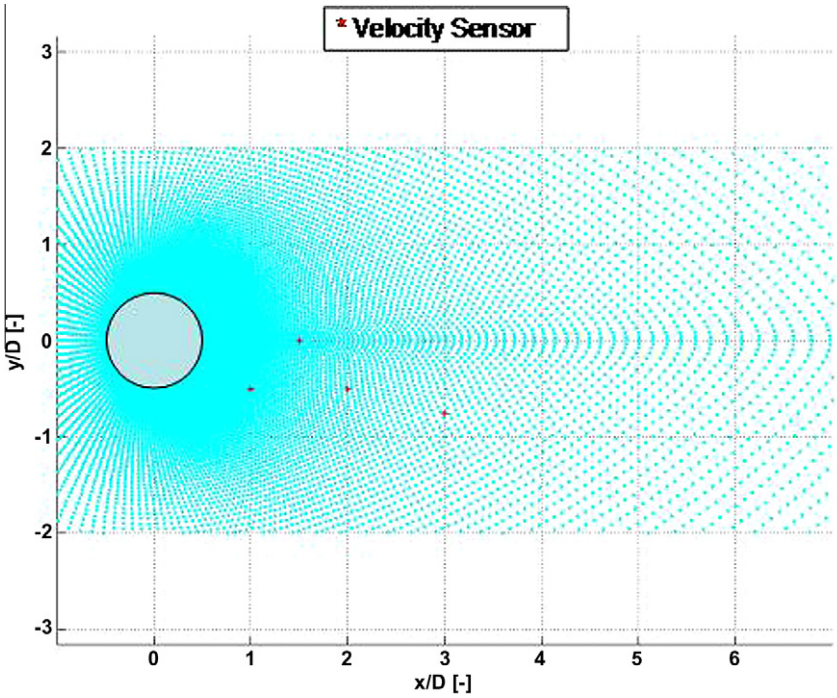

Fig. 4. Locations of the 4 Sensor configuration used in this study.

Table 2
Description of the information required for each of these estimation techniques. 4 sensors, $i = 1,\ldots,4$.

	QSE	DSE	ANNE
Linear terms	$S_i(t)$	$S_i(t)$	$S_i(t)$
Quadratic terms	"Auto" Terms: $S_i^2(t)$,"Cross" Terms: $S_1S_2(t)$, $S_1S_3(t)$, $S_1S_4(t)$ $S_2S_3(t)$ $S_2S_4(t)$ $S_3S_4(t)$	–	–

configurations is utilized. Only the streamwise velocity component was used for the sensor placement and number studies reported in this effort. The main idea in determining the sensor locations is to place the sensors on the extrema of the spatial modes in the wake as described in detail by Cohen et al. (2006b) Additionally, a small sensitivity study was conducted to obtain the final locations and number of the sensors for each of the sensor configurations examined. The locations of the sensors for the 4 sensor configurations studied (see Table 1 and Fig. 4) are referenced in terms of the CFD coordinates (the origin is at the center of the cylinder), non-dimensionalized with respect to the cylinder diameter, D, namely, x/D and y/D.

Now that the sensor number and location are determined, we develop an estimator based on an artificial neural network (ANN). The time histories of the mode amplitudes of the POD model are determined by mapping the flow field data onto the spatial modes using the least squares technique. The intent of the proposed strategy is that the velocity measurements provided by the sensors are processed by the estimator to provide the estimates of the 6 mode amplitudes of the DPOD model as follows: the mean flow, $\alpha_{1,1}$, the two fundamental von Kármán POD periodic modes, $\alpha_{2,1}$ and $\alpha_{3,1}$ and the three associated shift modes, namely, $\alpha_{2,1}$, $\alpha_{2,2}$ and $\alpha_{3,2}$. Only data concerning the streamwise component of the velocity was used for the sensor placement and number studies reported in this effort. The locations of the mode maxima/minima of the spatial modes of the DPOD model are used for sensor placement as described in detail by Cohen et al. (2006c) The criterion for quantifying the quality of the prediction is based on the RMS error of the prediction. We define the RMS error as the RMS of the error between the estimated modes based on sensor measurements (using any of the possible estimation techniques, ANNE for example) and the DPOD mode amplitudes obtained from the CFD simulation using the full flow field information. For sake of convenience, this RMS error, presented as a percentage, is normalized with the RMS of the exact mode amplitudes using the full flow field information.

In this effort,the estimation method of choice is based on a non-linear system identification approach described by Nelles[13]using Artificial Neural Networks (ANN) and ARX models (Nelles, 2001, Nørgaard et al., 2003).For the mapping of velocity measurements provided by the sensors onto the mode amplitudes of the six DPOD modes, the modified NNARXM (Neural Network Autoregressive, external input, Multi output) algorithm, originally developed by Nørgaard et al. (2003), is used as ANNE (Artificial Neural Network Estimation) (Nelles, 2001, Nørgaard et al., 2003).

The decision was to look into universal approximators, such as artificial neural networks (ANN), for their inherent robustness and capability to approximate any non-linear function to any arbitrary

Table 3
RMS of the Prediction Errors for six DPOD modes [%].

	Modes	1,1	2,1	3,1	1,2	2,2	3,2
TS	QSE	6.16	7.72	13.22	11.73	28.61	19.07
	DSE	19.33	14.37	16.73	18.92	36.74	45.08
	ANNE	0.19	9.86	6.61	9.67	11.90	12.38
VS1	QSE	13.99	15.60	23.08	17.03	40.48	33.73
	DSE	23.89	17.75	24.71	21.92	40.05	47.43
	ANNE	1.13	12.13	13.18	11.35	17.60	17.11
VS2	QSE	12.53	12.35	20.30	18.73	40.84	28.65
	DSE	23.56	14.99	21.39	20.99	44.75	47.88
	ANNE	0.86	12.37	10.54	10.62	19.04	19.44
VS3	QSE	11.76	15.59	20.85	12.81	36.23	25.98
	DSE	26.14	17.30	22.35	21.75	36.78	45.81
	ANNE	0.79	13.98	12.20	10.50	22.17	15.87
VS4	QSE	14.00	14.88	22.11	28.90	45.96	35.24
	DSE	25.08	16.91	22.51	24.96	55.18	56.23
	ANNE	1.54	16.26	14.66	14.11	29.55	27.13
VS5	QSE	9.28	15.44	21.38	38.97	83.60	75.70
	DSE	21.26	19.05	18.41	44.49	70.29	71.31
	ANNE	1.56	21.44	18.93	28.74	48.24	54.54
VS6	QSE	9.80	13.29	19.23	27.57	59.62	46.68
	DSE	22.19	16.70	17.21	33.96	54.98	54.26
	ANNE	1.17	16.45	13.03	18.35	30.10	32.10

degree of accuracy. The ANN, employed in this effort, in conjunction with the ARX model is the mechanism with which the dynamic model is developed using the POD mode amplitudes extracted from the CFD simulation. Non-linear optimization techniques, based on the back propagation method, are used to minimize the difference between the extracted POD mode amplitudes and the ANN while adjusting the weights of the model (Nørgaard et al., 2003). In order to assure model stability, the ARX dynamic model structure is incorporated. This structure is widely used in the system identification community (Nørgaard et al. (2003)). A salient feature of the ARX predictor is that it is inherently stable even if the dynamic system to be modeled is unstable. This characteristic of ARX models often lends itself to successful modeling of unstable processes as described by Nelles (2001).

ANNE, based on the Multilayer Perceptron Neural Network, uses an adequate training set as described in Fig. 2. The ANN network is designed and then the "frozen" ANN design, with its associated weighing matrices, is validated with new data. The purpose is to obtain a robust and real-time estimator for as low a number of sensors as possible for application to wake control.

The artificial neural network (ANN) has the following features:

Input Layer: No past outputs; 4 sensors each having: 8 past inputs each with "current time" signal +3 time delays, i.e. $\sim 1/8$ ofa shedding cycle per input. 65 Neurons ($4 \times 4 \times 4 + 1$ bias = 65) in the input layer.

Hidden Layer: One hidden layer consisting of 6 neurons. The activation function in the hidden layer is based on the non-linear *tanh* function. A single bias input has been added to the output from the hidden layer.

Output Layer: Six outputs, namely, the 6 DPOD mode amplitudes: the mean flow, $\alpha_{1,1}$, the two fundamental von Kármán POD periodic modes, $\alpha_{2,1}$ and $\alpha_{3,1}$and the three associated shift modes, namely, $\alpha_{2,1}$, $\alpha_{2,2}$and $\alpha_{3,2}$. The output layer has a linear activation function.

Weighting Matrices: The weighting matrices between the input layer and the hidden layer (W_1) and between the hidden layer and the output layer (W_2) depend on the number of sensors. For example, for the single sensor case $W_1$is of the order of $[65 \times 6]$ and $W_2$is of the order of $[7 \times 6]$. These weighting matrices are initialized randomly.

Training the ANN: Back propagation, based on the Levenberg–Marquardt algorithm, was used to train the ANN using the toolbox by Nørgaard et al.[13] The training procedure converged in approximately 100 iterations. The training data is based on the design case as illustrated in Fig. 2. The training set contained 1500 snapshots. Sinusoidal forcing, at the

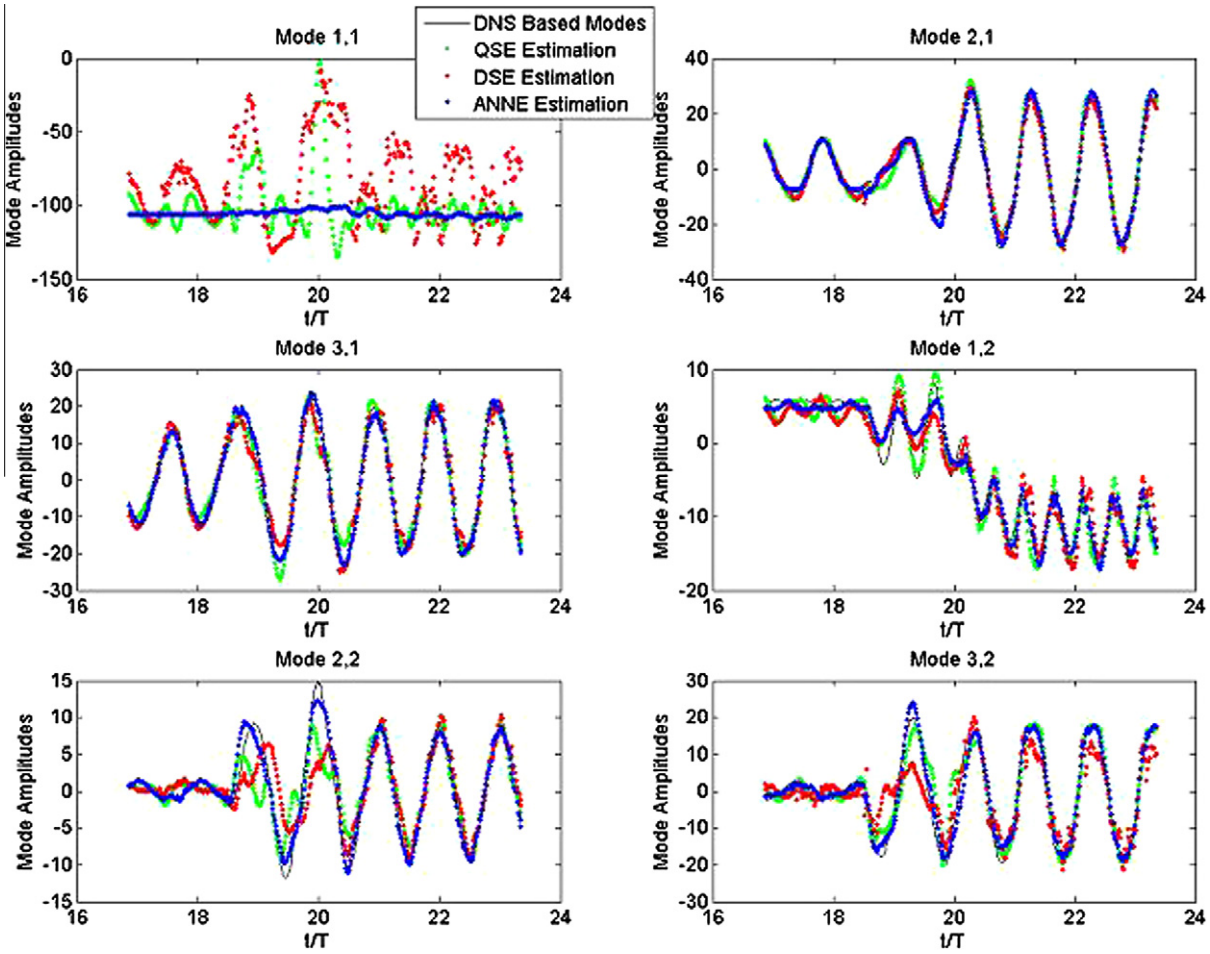

Fig. 5. Mode amplitudes the 6 DPOD modes for the Training data set, TS: $f/f0 = 1$ and A/D = 0.25. Forcing activated at $t/T = 18$ and stopped at $t/T = 33$, after 15 full forcing cycles.

fundamental Strouhal frequency and a constant amplitude of $y_{cyl}/D = 0.25$, is introduced only after the first 180 snapshots and stopped after exactly 15 full forcing cycles. The remaining 429 snapshots are then unforced.

Validating the ANN: Six different validation data sets were used to represent the off-design cases as illustrated in Fig. 2. Each of the validation sets contained 1500 snapshots and includes sinusoidal forcing, at the frequency and constant amplitude described in Fig. 2, introduced after the first 180 snapshots and stopped after exactly 15 full forcing cycles. The remaining 429 snapshots are then unforced.

5. Comparison of ANNE to other techniques

The results obtained for the training and validation set for ANNE will be compared to other state-of-the-art techniques used by the flow control community. Recent work by Cohen, Siegel, Seidel, and Mclaughlin (2006d) shows that effective suppression of the cylinder wake is possible with feedback based on the first periodic DPOD mode, Mode 2,1 and its shift mode, Mode 2,2. We believe that effective feedback should be possible using the first three modes and their associated shift modes. For this comparative study between three different estimation techniques, the sensor configuration described in the previous section is examined. These techniques are as follows:

1. Quadratic Stochastic Estimation (QSE) is based on a modified LSE technique. This modification, which includes quadratic terms, was proposed by Murray and Ukeiley (2002) as well as by Ausseur et al. (2006)
2. Dynamic Stochastic Estimation (DSE), which includes 3 time delays as additional inputs to that at time t (for a total of 4 input signals per sensor), along the lines examined by Debiasi et al. for the cavity acoustic suppression problem (2006)
3. Artificial Neural Network Estimation (ANNE) as developed in this paper.

In Table 2, the information required for each of these estimation techniques is presented. The DSE and ANNE require exactly the same amount of information. The results for the three estimation techniques are presented in Table 3. Table 3 presents the RMS of the prediction errors, as defined in the previous section, for six DPOD modes [%]. We can see that the RMS of these errors for ANNE is lower by an order of magnitude for Mode 1,1 and about 50% better for the higher modes when compared to the DSE and the QSE techniques.

Fig. 5 provides the predicted mode amplitudes compared to the DNS based modes for the training data set, TS ($f/f_0 = 1$ and A/D = 0.25 as shown in Fig. 2). For Figs. 5–7 it needs to be noted that the forcing is activated at $t/T = 18$ and stopped at $t/T = 33$, after 15 full forcing cycles. Also, for the sake of clarity, in Figs. 5–7, only six

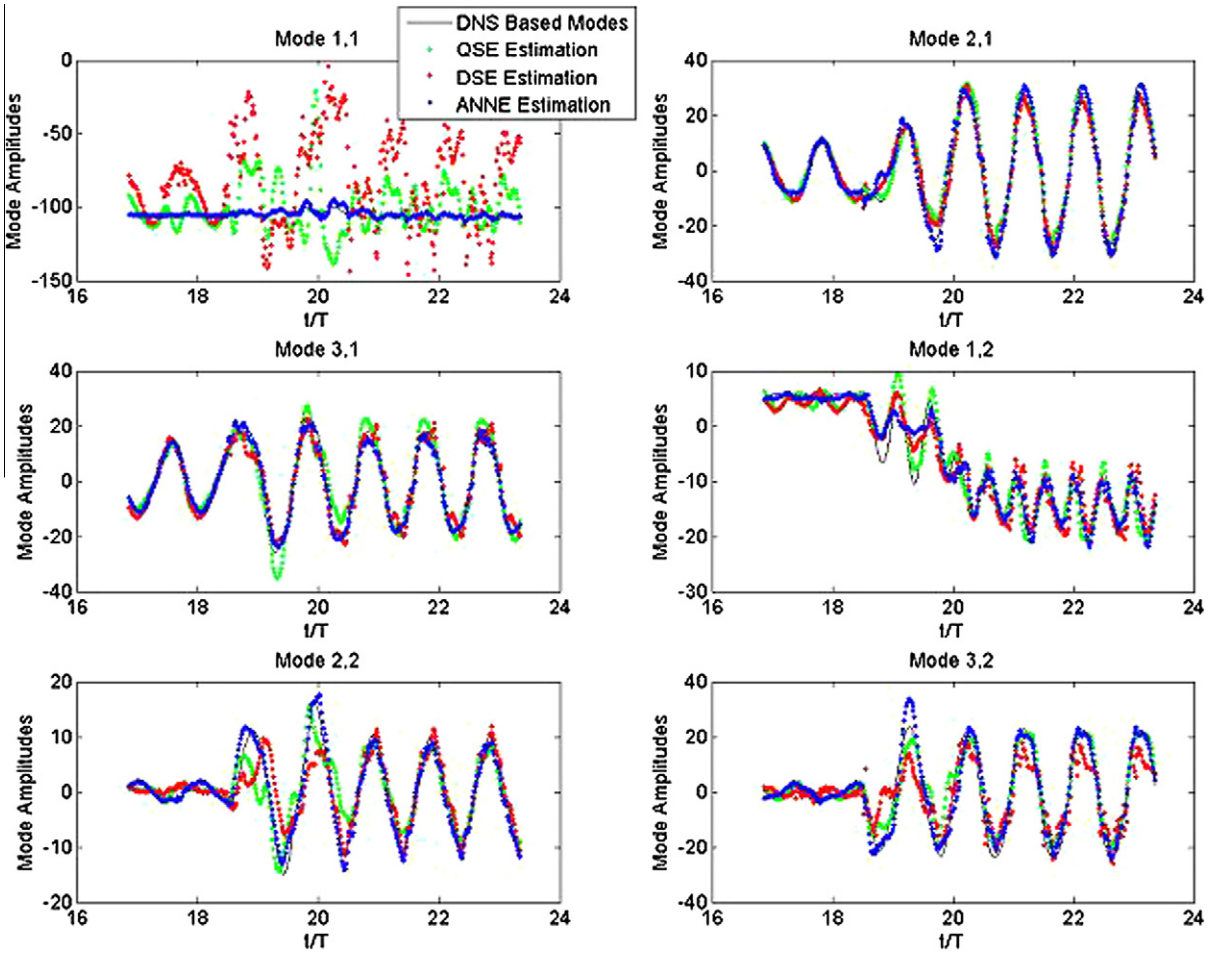

Fig. 6. Mode amplitudes the 6 DPOD modes for the validation data set, VS3: $f/f0 = 1.05$ and A/D = 0.30. Forcing activated at $t/T = 18$ and stopped at $t/T = 33$, after 15 full forcing cycles.

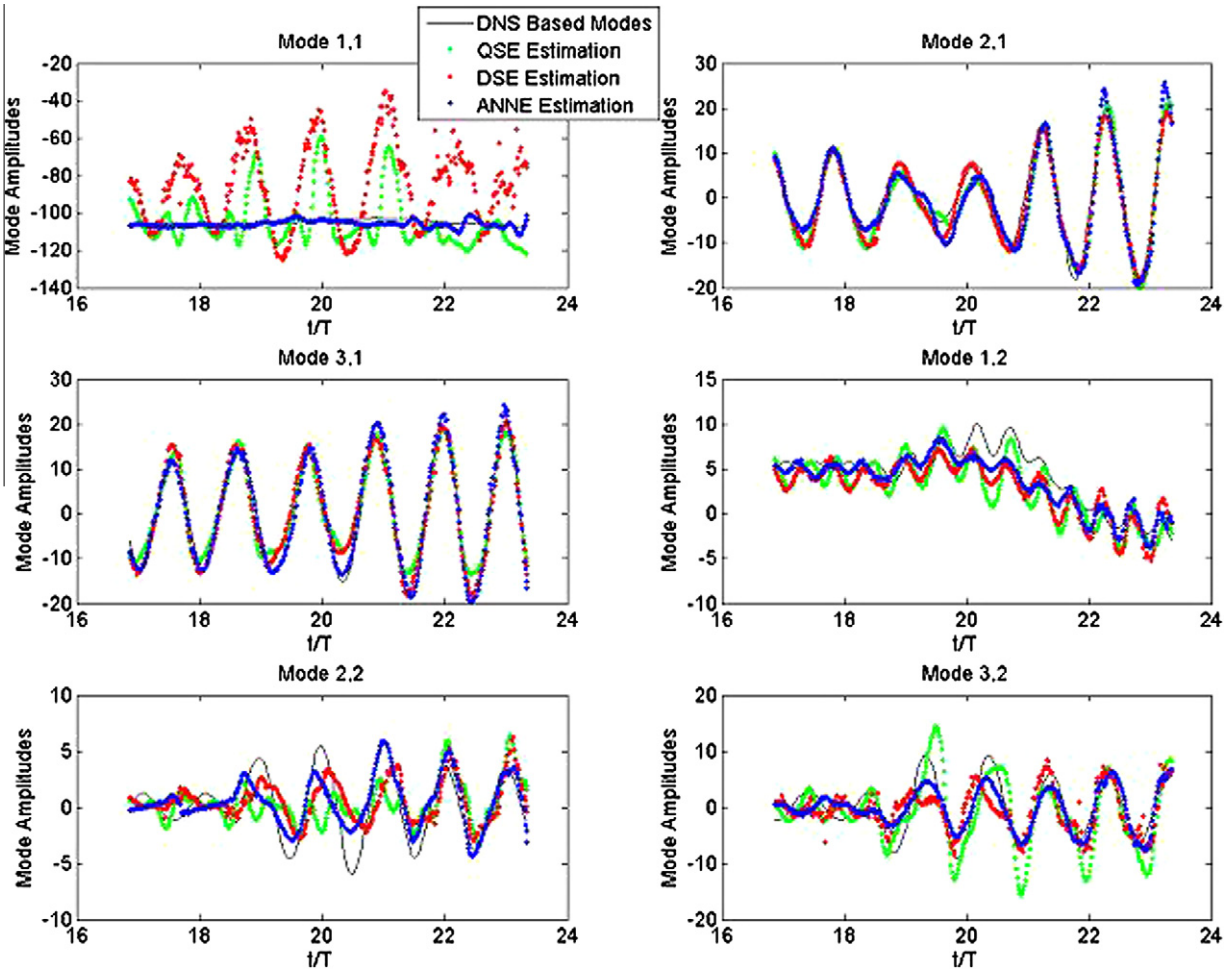

Fig. 7. Mode amplitudes the 6 DPOD modes for the validation data set, VS5: $f/f0 = 1.0$ and A/D = 0.10. Forcing activated at $t/T = 18$ and stopped at $t/T = 33$, after 15 full forcing cycles.

shedding cycles are plotted. Nevertheless, the RMS Error calculation is based on all 24 shedding cycles which includes initiation of forcing after 2 shedding cycles and the cessation of the forcing after 15 full forcing cycles. Figs. 6 and 7 provide the predicted mode amplitudes compared to the CFD based modes for the validation data set VS3 ($f/f_0 = 1.05$ and A/D = 0.30) and validation data set VS3 ($f/f_0 = 1.0$ and A/D = 0.10), respectively. Thus, VS3 constitutes a validation case that differs in frequency, while VS3 is a validation case at the natural shedding frequency, but at an amplitude that is just at the limit of lock-in. While for the VS3 case all techniques provide reasonably accurate estimates for the unforced, transient and open loop forced flow states, this is not the case for the VS5 results. There, both DSE and QSE produce higher harmonic frequencies during the transient flow state, as can be seen best in the Mode 22 and Mode 32 plots in Fig. 7. While only two of the transient validation cases are shown, the other validation cases look qualitatively similar. The RMS errors for these cases are also comparable, as shown in Table 3.

Based on the results shown in Table 3 and Figs. 5–7, the following observations can be made:

1. The estimation error for the training cases for each of the 6 modes is lower than in the validation cases.
2. ANNE provides superior results for the sensor configuration studied. The improvement in performance in ANNE may be attributed to a combination of both non-linear mapping and dynamic memory. This is in contrast to DSE, which does use only dynamic data but does not account for nonlinearities, and QSE, which captures some nonlinear effects, but has no dynamic data input.
3. There are three parameters one would like to observe in a good prediction and we mentioned one of those being the RMS error. Additionally, for the periodic modes, such as the von Kármán shedding modes 2,1 and 3,1, we would also need to consider the frequency and phase prediction as well. It is interesting to note that both frequency and phase for the von Kármán fluctuating modes are relatively well predicted by all three techniques. The main differences are in the amplitude predictions of the three different techniques, which are also important when considering feedback control.
4. It is interesting to note the differences in performance for mode 1,1. This is an important mode since it contains most of the "modal energy". ANNE provides DPOD time coefficient estimation with RMS errors which are an order of magnitude lower than the errors obtained with DSE and QSE. The discrepancy may be attributed to scaling limitations in the way DSE and QSE were implemented.

6. Conclusion

Based on a previous sensor placement study (Cohen et al. (2006c)), a comparison was made between the effectiveness of the conventional DSE and QSE techniques versus the newly proposed ANNE for real-time estimation of the low-dimensional

Double Proper Orthogonal Decomposition (DPOD) states based on four flow field velocity measurements. The development of the procedure used CFD simulation data of a cylinder at a Reynolds number of 100. We introduce DPOD as a means to derive POD spatial modes that span different flow conditions. For the estimation of the first six DPOD modes, we show that a four sensor configuration using ANNE provides lower estimation errors (order of magnitude for Mode 1,1 and about 50% for the higher modes) when compared to conventional state-of-the-art techniques appearing in literature. We attribute the augmented performance exhibited by ANNE to both its non-linear modeling capability as well as the dynamic behavior due to the inclusion of the time lag terms. This is demonstrated by comparing ANNE to two other techniques, namely, QSE and DSE, which are being proposed by other researchers in the field. Comparisons were not made to the LSE technique since this technique, although examined, provided unfeasible estimates.

7. Outlook

The next step in the research is to examine the effectiveness of ANNE in a closed-loop application, both in high resolution simulations and in experiments. Additional studies may include the following investigations:

- Assess the sensitivity of the number and location of sensors to transient excitation of the forced cylinder wake.
- For the case of transient forcing, we will systematically and quantitatively examine the main contributors to this betterment of performance, namely: nonlinearity vs. linearity; dynamic mapping (“delay” or memory) vs. static mapping; and robustness to noise.
- Examine the generic nature of the developed strategy (ANNE) for surface mounted sensor configurations based on pressure or skin friction measurements.
- Examine the sensitivity of the ANN architecture to performance vs. computational cost for all the above cases.

Acknowledgments

The authors thank Lt. Col. Scott Wells, Lt. Col. Sharon Heise (AFOSR), and Dr. James Myatt (AFRL) for their support and assistance. The authors acknowledge the assistance of Dr. Jim Forsythe of Cobalt Solutions, LLC and Dr. Young Sug-Shin of Agency for Defense Development (ADD), South Korea.

References

Adrian, R. J. (1977). *On the role of conditional averages in turbulence theory. Proceedings of the fourth biennial symposium on turbulence in liquids*. Princeton: Science Press.

Ausseur, J.M., Pinier, J.T., Glauser, M.N., Higuchi, H., & Carlson, H. (2006). Experimental development of a reduced-order model for flow separation control. AIAA Paper 2006-1251.

Cohen, K., Siegel, S., & Mclaughlin, T. (2004). Control issues in reduced-order feedback flow control, Invited Lecture at session titled Closed-Loop Flow Control: Algorithms and Applications. AIAA Paper 2004-0575.

Cohen, K., Siegel, S., Seidel, J., & Mclaughlin, T. (2006). Low dimensional modeling, estimation and control of a cylinder wake. In *Invited lecture at Invited Session organized by Dr. James Myatt of AFRL/VA called Order Reduction and Control for Aerodynamics, 45th IEEE Conference on Decision and Control*.

Cohen, K., Siegel, S., Seidel, J., & Mclaughlin, T. (2006B). Reduced order modeling for closed-loop control of three dimensional wakes. AIAA Paper 2006-3356.

Cohen, K., Siegel, S., & Mclaughlin, T. (2006c). A heuristic approach to effective sensor placement for modeling of a cylinder wake. *Computers and Fluids, 35*(1), 103–120.

Cohen, K., Siegel, S., Seidel, J., & Mclaughlin, T. (2006D). Low dimensional modeling, estimation and control of a cylinder wake. In *Invited lecture at Session “Order Reduction and Control for Aerodynamics, 45th IEEE Conference on Decision and Control*.

Cohen, K., Siegel, S., Seidel, J., Aradag, S., & Mclaughlin, T. (2007). Nonlinear estimation of transient flow field low dimensional states using double proper orthogonal decomposition. AIAA 2007-2836.

Debiasi, M., Little, J., Caraballo, E., Yuan, X., Serrani, A., Myatt, J.H., & Samimy, M. (2006). Influence of stochastic estimation on the control of subsonic cavity flow – A preliminary study. AIAA-2006-3492.

Gillies, E. A. (1998). Low-dimensional control of the circular cylinder wake. *Journal of Fluid Mechanics, 371*, 157–178.

Holmes, P., Lumley, J. L., & Berkooz, G. (1996). *Turbulence, Coherent Structures, Dynamical Systems and Symmetry*. Cambridge: Cambridge University Press.

Koopmann, G. (1967). The vortex wakes of vibrating cylinders at low Reynolds numbers. *Journal of Fluid Mechanics, 28*(3), 501–512.

Ljung, L. (1999). *System Identification: Theory for the User* (second ed.). Upper Saddle, NJ, USA: Prentice Hall.

Min, C., & Choi, H. (1999). Suboptimal feedback control of vortex shedding at low Reynolds numbers. *Journal of Fluid Mechanics, 401*, 123–156.

Murray, N.E., & Ukeiley, L.S. (2002). Estimating the shear layer velocity field above an open cavity from surface pressure measurements. AIAA Paper 2002-2866.

Nelles, O. (2001). *Nonlinear System Identification*. Berlin, Germany: Springer-Verlag.

Noack, B.R., Tadmor, G., and Morzynski, M. (2004). Low-dimensional models for feedback flow control. Part I: Empirical Galerkin models. AIAA Paper 2004-2408.

Noack, K., Afanasiev Morzynski, M., & Thiele, F. (2003). A hierarchy of low dimensional models for the transient and post-transient cylinder wake. *Journal of Fluid Mechanics, 497*, 335–363.

Nørgaard, M., Ravn, O., Poulsen, N. K., & Hansen, L. K. (2003). *Neural Networks for Modeling and Control of Dynamic Systems*. London, U.K: Springer-Verlag. 3rd printing.

Oertel, H. Jr., (1990). Wakes behind blunt bodies. *Annual Review of Fluid Mechanics, 22*, 539–564.

Panton, R. L. (1996). *Incompressible Flow* (second ed.). New York: John Wiley & Sons.

Park, D. S., Ladd, D. M., & Hendricks, E. W. (1993). Feedback control of a global mode in spatially developing flows. *Physics Letters A, 182*, 244–248.

Roussopoulos, K. (1993). Feedback control of vortex shedding at low Reynolds numbers. *Journal of Fluid Mechanics, 248*, 267–296.

Shin, Y., Cohen, K., Siegel, S., Seidel, J., & Mclaughlin, T. (2006). Neural network estimator for closed-loop control of a cylinder wake. AIAA Paper 2006-6428.

Siegel, S., Cohen, K., Seidel, J., & Mclaughlin, T. (2005). Short time proper orthogonal decomposition for state estimation of transient flow fields. AIAA Paper 2005-0296.

Siegel, S., Cohen, K., & Mclaughlin, T. (2006). Numerical simulations of a feedback controlled circular cylinder wake. *AIAA Journal, 44*(6), 1266–1276.

Siegel, S., Cohen, K., Seidel, J., & Mclaughlin, T. (2006B). State estimation of transient flow fields using double proper orthogonal decomposition (DPOD). presented at the International Conference on Active Flow Control, Berlin, Germany.

Sirovich, L. (1987). Turbulence and the dynamics of coherent structures Part I: Coherent structures. *Quarterly of Applied Mathematics, 45*(3), 561–571.

Strang, W.Z., Tomaro, R.F., Grismer, M.J. (1999). The Defining Methods of Cobalt60: A Parallel, Implicit, Unstructured Euler/Navier–Stokes Flow Solver. AIAA 99-0786.

Williamson, C. H. K. (1996). Vortex dynamics in the cylinder wake. *Annual Review on Fluid Mechanics, 8*, 477–539.